

## Reconstruction of 3D myocardial fiber architecture using SENSE-DTI at 3 Tesla

P. Schmid<sup>1</sup>, T. Jaermann<sup>1</sup>, U. Gamper<sup>1</sup>, P. P. Lunkenheimer<sup>2</sup>, P. Boesiger<sup>1</sup>, P. Niederer<sup>1</sup>

<sup>1</sup>Institute for Biomedical Engineering, ETH and University Zurich, Zurich, Switzerland, <sup>2</sup>Experimental Surgery, University of Muenster, Muenster, Germany

### Introduction

There is abundant evidence that ventricular structure and function (1-4) are markedly inhomogeneous. Nonetheless, it is commonly assumed that ventricular emptying is an effect of the centripetal constriction of the prevailing surface-parallel myocardial array which wraps the ventricular cavity (5, 6). However, though the existence of a three-dimensional netting of the heart muscle has never been called into question its functional impact has been virtually excluded from discussion.

Myocardial fiber structure correlates with anisotropy in the water self-diffusion of the myocardium (7), which can be assessed by using Diffusion Tensor MRI (DTI) (8, 9). Measuring the 3D diffusion properties in each voxel of a complete heart allows visualizing myocardial fiber structure, following the direction of the eigenvector corresponding to the largest eigenvalue. One of the most prominent advantage of this method is that once the data are acquired, they can be analysed repetitively with focus variable architectural aspects.

The aim of the present study is to explore the heart muscle's fibre structure using DTI, enabling the depiction of fibre architecture to an extent which exceeds most advanced histological techniques.

### Methods

From eight porcine hearts obtained from a local slaughterhouse immediately after slaughter the subepicardial fat, the coronary vessels, the atria, and the papillary muscles were removed to reduce image artefacts. The hearts were housed in a plastic box (11 x 11 x 12 cm<sup>3</sup>), filled with agarose (2 %) gel which was doped with copper sulfate (0.5 %) to obtain better signal contrast between myocardium and the surrounding gel. Care was taken that while filling up the ventricular cavities with gel the inclusion of air bubbles was omitted between the grooved inner contours.

**Diffusion tensor imaging:** The measurements were performed on a 3T Philips Intera whole body MR system (Philips Medical Systems, Best, NL) using a surface coil array consisting of four rectangular elements for signal reception. A multi-slice Stejskal-Tanner sequence was used to obtain diffusion weighting in six independent directions. Images were acquired using single-shot echo-planar imaging (EPI) in combination with the parallel imaging technique Sensitivity Encoding (SENSE) (10) to reduce EPI-related artefacts (11). Imaging parameters were: FOV = 130 x 130 mm<sup>2</sup>, 80 x 80 image matrix, SENSE-factor = 1.9 (in-plane spatial resolution = 1.62 x 1.62 mm<sup>2</sup>), slice thickness = 2 mm, TR = 10.2 s, TE = 70 ms, flip angle  $\alpha$  = 90°, number of signal averages = 9, diffusion gradient = 3.1 G/cm (b = 900 s/mm<sup>2</sup>). A 3D volume of 43 adjacent short axis slices was acquired covering the entire heart. Thereby the total measurement duration was about 20 min. For validation purposes, diffusion weighted images of a papillary muscle which exhibits a well defined longitudinal fiber orientation were also collected and analyzed separately.

**Fiber reconstruction:** The six diffusion weighted images were segmented and registered using a 2D affine image registration algorithm (12) to correct for residual image distortions due to eddy currents. On a voxel by voxel basis the diffusion tensor's properties were derived by singular value decomposition. The fibers were reconstructed using a custom-made backward trilinear tensor tracking algorithm.

### Results

The histology and the diffusion-weighted image of the papillary muscle is shown in Fig. 1a. The color indicates a uniform fiber orientation in the longitudinal direction as known from histological examinations. When looking to the bi-ventricular base from the apex on Fig. 1b, with the thick-walled left ventricle on the right, the thin-walled right ventricle on the left, the orientation of the imaged diffusive pathways is in compliance with established knowledge on fibre orientation as known from histology (1, 2). The prevailing alignment follows a circular course with some subepicardial layers radiating in a clockwise turn from outside to inside. The same results can be observed when measuring a sequence of short axis slices from the apex to the base and reconstruction of the myocardial fibres following the largest diffusion eigenvalues in each voxel (Fig. 1c).

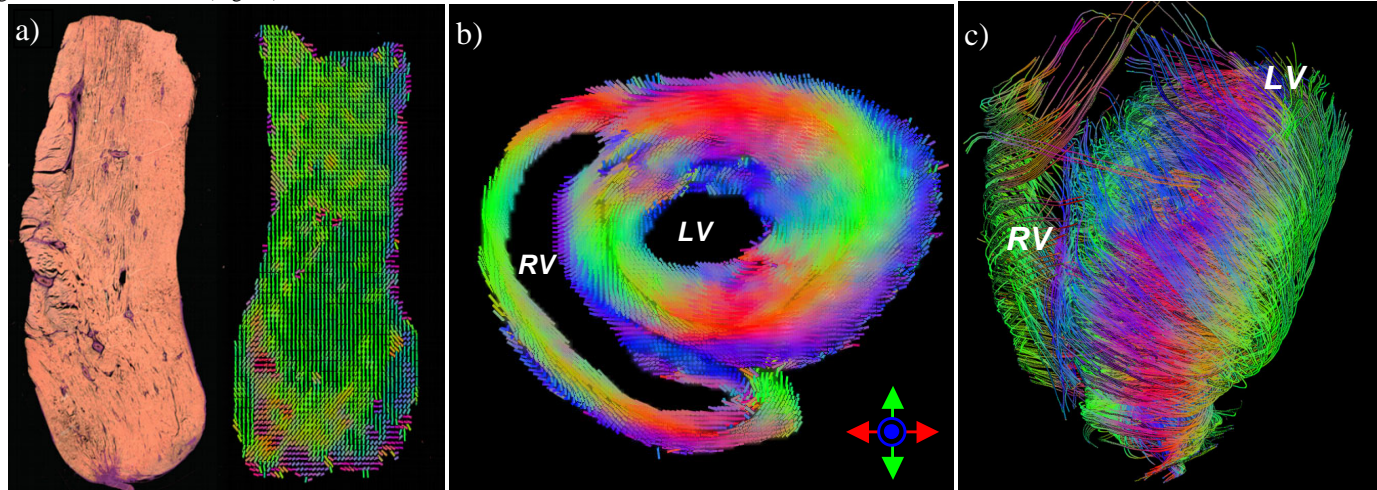


**Fig1:** a) Histology and DTI based fiber orientation of the papillary muscle. b) Short axis slice at basal level revealing the local main diffusion directions. The colors correspond to the main diffusion orientations as indicated at bottom right. c) 3D-Reconstruction of the muscle fiber architecture in the whole heart (LV: Left ventricle, RV: Right ventricle).

### Discussion:

The excellent correspondence of papillary fiber orientation detected using SENSE-DTI with data from histology indicates the validity of the methods used. Fiber orientations reconstructed for both ventricles of the pig heart were in accordance to previous histological examinations. It is concluded that DTI at high field strength incorporating parallel imaging allows accurate reconstruction of global fiber structure in ex-vivo samples with reasonably short measurement times. The method holds great potential in complementing histological examinations used to study changes of cardiac fiber orientations associated with a variety of diseases.

**References** 1. Streeter DD Jr et al.; Handbook of Physiology, American Physiological society 1990; Bethesda, Maryland. 2. Anderson RH et al. in Cardiac Anatomy, London: Churchill Livingstone 1980; 5.14-5.26. 3. Grant RP et al.; Circulation 1965; 32, 301-308. 4. Sanchez-Quintana D et al.; Acta Anatomica 1990; 138, 352-358. 5. Bovendeerd PHM et al.; J. Biomech 1994; 27, 941-51. 6. Nielsen PMF et al.; Am. J. Physiol. 1991; 260, H1365-H1378. 7. Hsu EW et al. Am J Physiol 1998; 274, H1627-H1634. 8. Reese TG et al.; Magn Reson Med 1995; 34(6): 786-91. 9. Tseng WY et al.; J Magn Reson Imaging 2003; 17(1):31-42. 10. Pruessmann KP et al.; Magn Reson Med 1999; 42: 952-962. 11. Jaermann T et al.; Magn Reson Med, in press. 12. Netsch T et al.; Proc. ICCV 2001: 718-725.